

**Electronic Supporting Information**

*belonging to*

**A Magnetic Iron(III) Switch with Controlled and Adjustable Thermal Response  
for Solution Processing**

**UV-vis measurements.** Temperature-dependent UV-vis spectra for all complexes **1** and **2** are shown in Figures S1-S4 and reveal an isosbestic point at 580 nm. At room temperature (298 K), the extinction at 650 nm is essentially zero and indicates the presence of HS species exclusively (Table S1).<sup>S1</sup> At lower temperature,  $\epsilon_{650}$  therefore gives an estimate of how large the LS portion is relative to the other complexes investigated here. The reduction of  $\epsilon_{500}$  provides a rough estimate of the decrease of the HS species upon cooling. Because  $\epsilon_{500}$  of the LS species is unknown, this estimate correlates reasonably well with the increase of  $\epsilon_{650}$  and hence, these values allow for a relative classification of the completeness of the SCO events reported here. To obtain a plot of the spin conversion over temperature (Figure 2 main text)  $\gamma'$  was introduced to indicate the SCO completeness of the fraction of complexes that actually undergo spin transition.  $\gamma'$  is derived from  $\epsilon_{650}$  and is 0 at 170 K, where no further spin transition was observed for all complexes that were functionalized with C<sub>18</sub>H<sub>37</sub> or longer tails and  $\gamma'_{\text{HS}} = 1$  at room temperature.

---

1 For the functionalized complexes **1b–g** and **2** complexes the absorbance maxima at ~380 nm is also indicative of the LS state as it varies like the band at 650 nm. Complex **1a** is different, a band at 330 nm band at RT shifts to 347 nm at 170 K. Such charge transfer and intraligand transition at ~380 nm has metal character since dependent on the electronic configuration of the metal center.

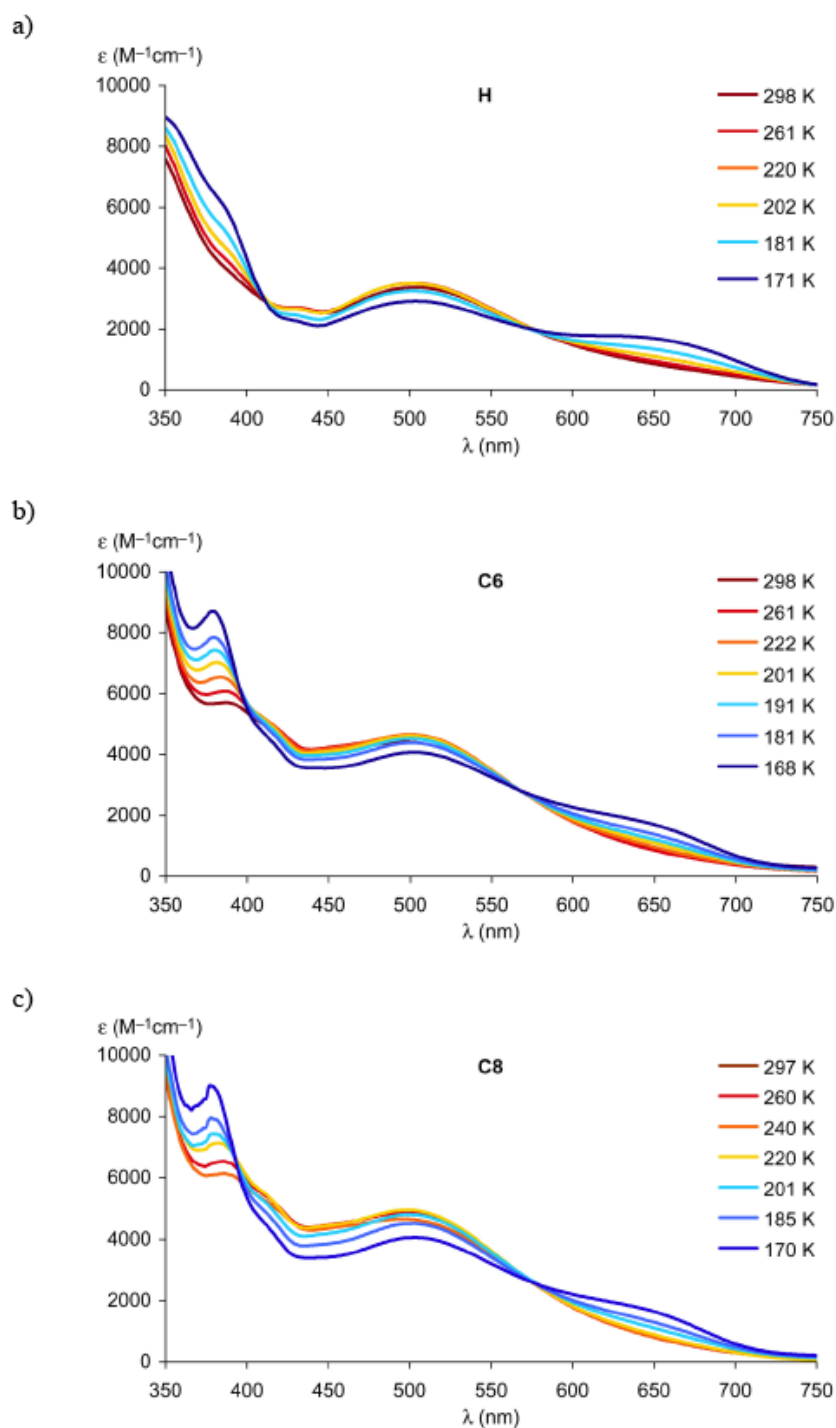


**Figure S1.** Temperature-dependent UV spectra for unfunctionalized complexes (a) **1a** and for complexes with linear alkyl chains: (b) **1b**, (c) **1c** (0.2 mM in  $CH_2Cl_2$ ).

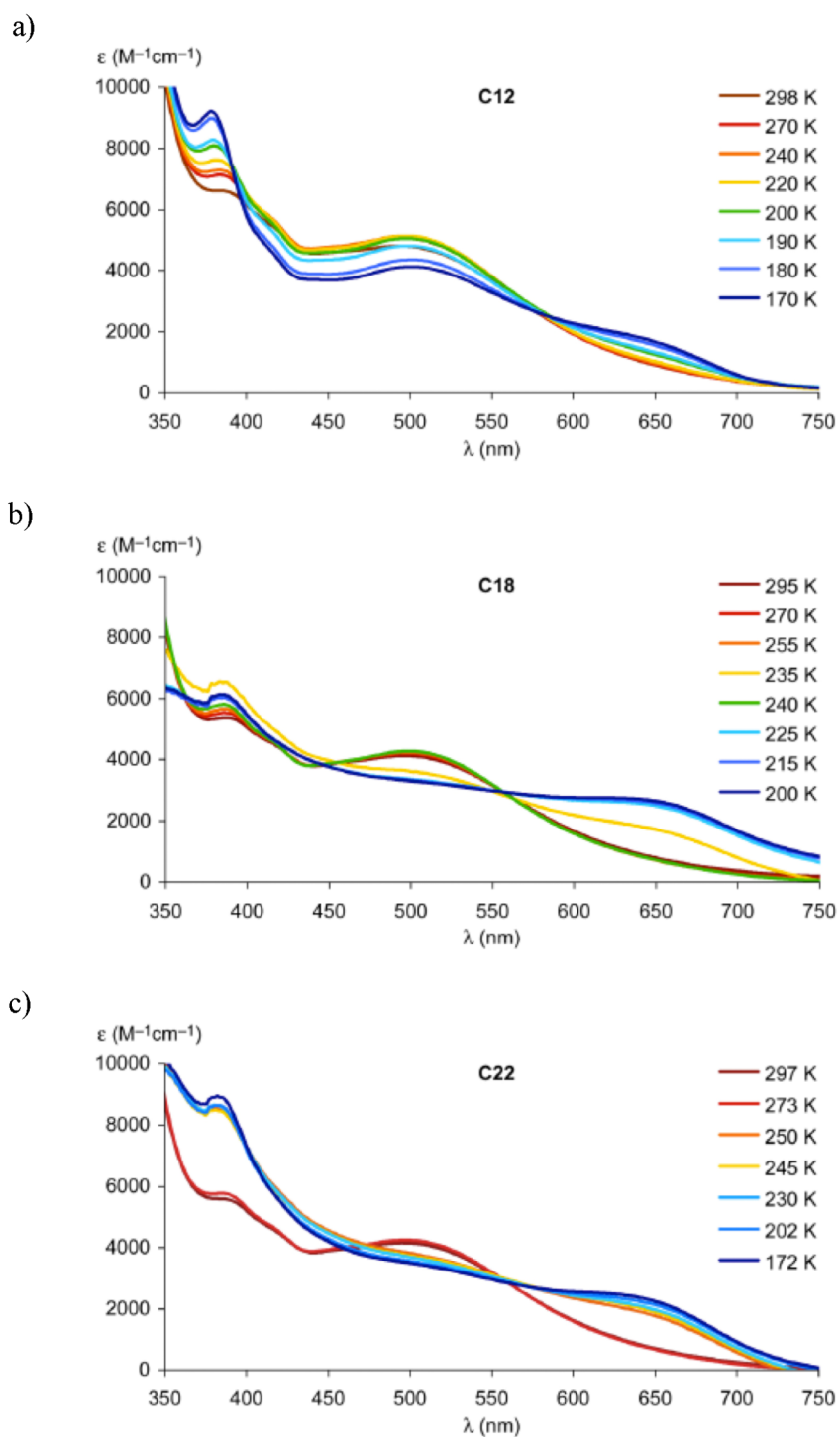


**Figure S2.** Temperature-dependent UV spectra for complexes (a) **1d**, (b) **1e**, and (c) **1f** (0.2 mM in  $CH_2Cl_2$ ).

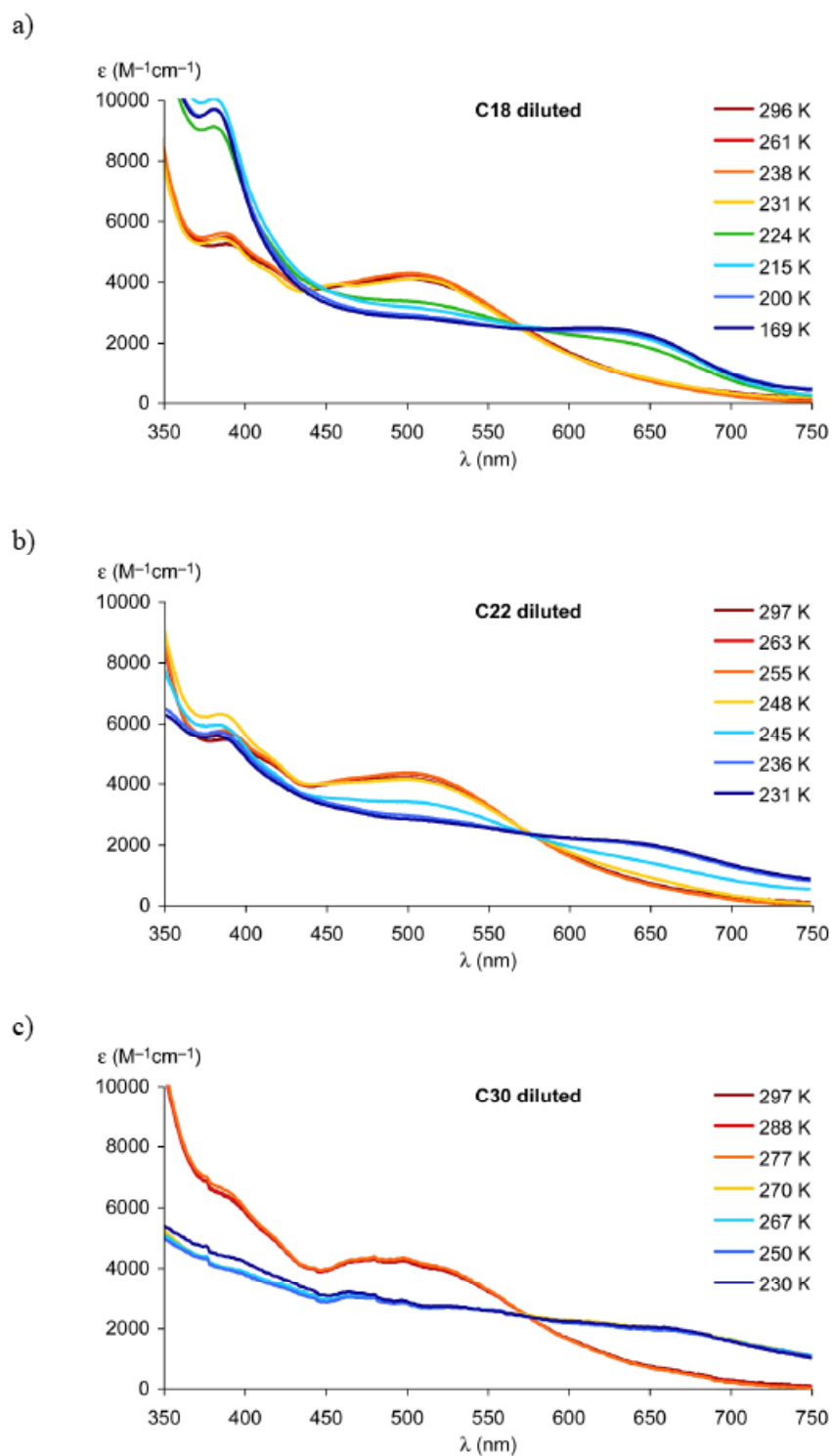


**Figure S3.** Temperature-dependent UV spectra for linear chain complexes (a) **1e**, (b) **1f**, and (c) **1g** in  $CH_2Cl_2$  at 0.04 mM.

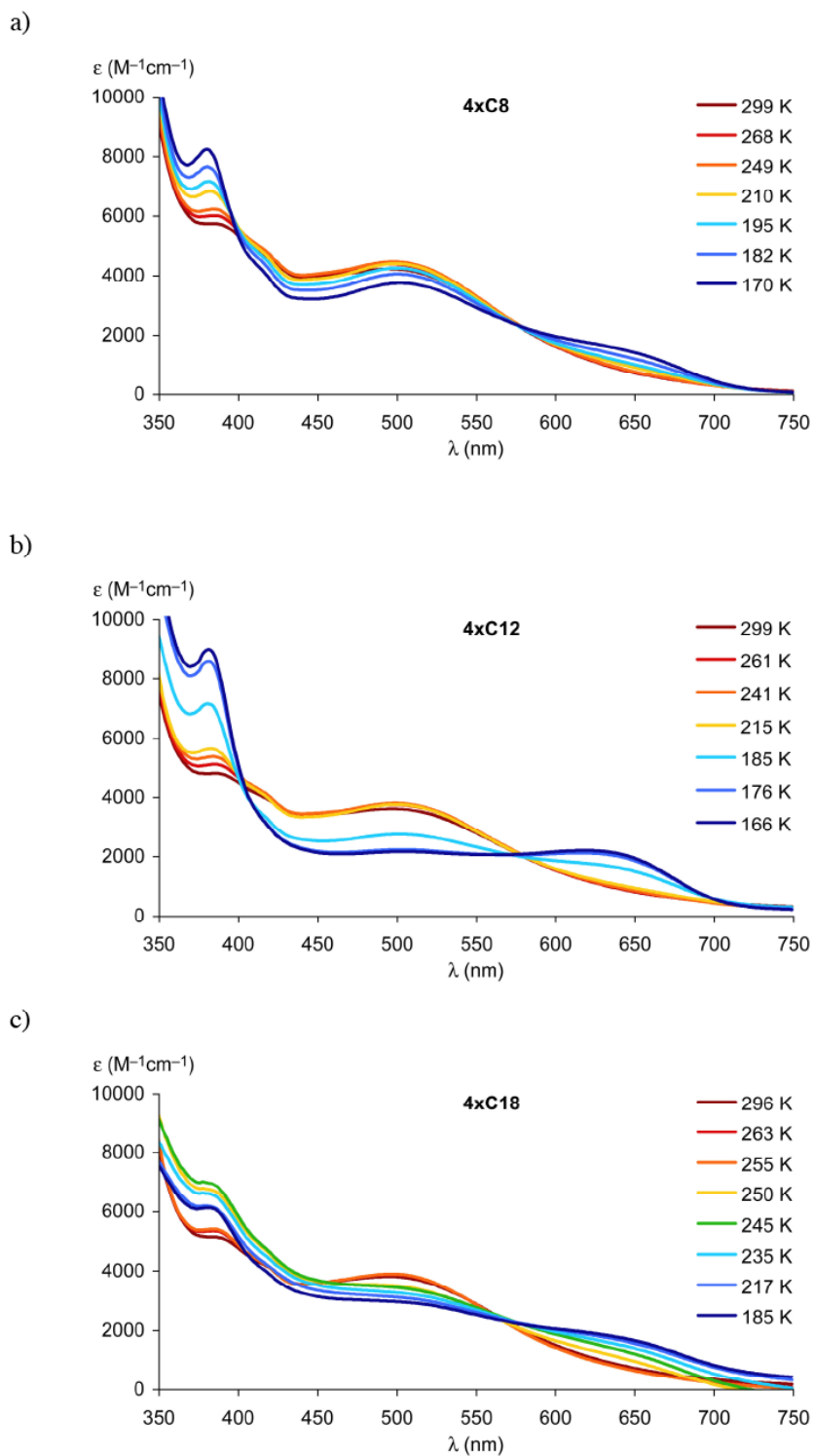


**Figure S4.** Temperature-dependent UV spectra for four chain complexes (a) **2c**, (b) **2d**, and (c) **2e** in  $CH_2Cl_2$  at 0.2 mM.

**Table S1.** Temperature-dependent UV-vis data for complexes **1** and **2**.<sup>a</sup>

complex	R group	$\epsilon_{500}(298\text{K})$	$\epsilon_{500}(170\text{ K})$	$\epsilon_{650}(170\text{ K})$	$T_{\text{SCO}}(\text{K})$ <sup>b</sup>
<b>1a</b>	H	3290	2840	1670	187
<b>1b</b>	OC <sub>6</sub> H <sub>13</sub>	4350	3980	1730	187
<b>1c</b>	OC <sub>8</sub> H <sub>17</sub>	4610	3980	1680	191
<b>1d</b>	OC <sub>12</sub> H <sub>25</sub>	4760	4070	1720	194
<b>1e</b>	OC <sub>18</sub> H <sub>37</sub>	4070	3260	2740	235
<b>1f</b>	OC <sub>22</sub> H <sub>45</sub>	4100	3480	2280	253
<b>1g</b> <sup>c</sup>	OC <sub>30</sub> H <sub>61</sub>	4200	2870 <sup>d</sup>	2020 <sup>d</sup>	275
<b>2c</b>	2 × C <sub>8</sub> H <sub>17</sub>	4180	3680	1450	190
<b>2d</b>	2 × C <sub>12</sub> H <sub>25</sub>	3460	2000	1890	189
<b>2e</b>	2 × C <sub>18</sub> H <sub>37</sub>	3900	3030 <sup>e</sup>	1740 <sup>e</sup>	246

<sup>a</sup> Solution in CH<sub>2</sub>Cl<sub>2</sub> (0.2 mM);  $\epsilon$  in M<sup>-1</sup>cm<sup>-1</sup>. <sup>b</sup> Spin crossover temperature determined at  $\gamma'_{\text{HS}} = 0.5$  upon cooling. <sup>c</sup> Solution in CH<sub>2</sub>Cl<sub>2</sub> (0.04 mM). <sup>d</sup> At 230 K. <sup>e</sup> At 185 K.

Plots of the temperature-dependent magnetic change upon dilution are shown in Figure S5, and the dependence on the number of alkyl chains are shown in Figure S6.

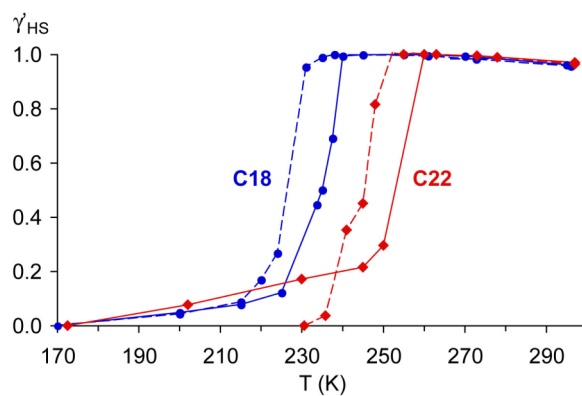


**Figure S5.** Plot of the high-spin fraction of iron complexes **1e** (blue) and **1f** (red) at 0.2 mM (solid lines) and at 0.04 mM concentration (dashed lines).

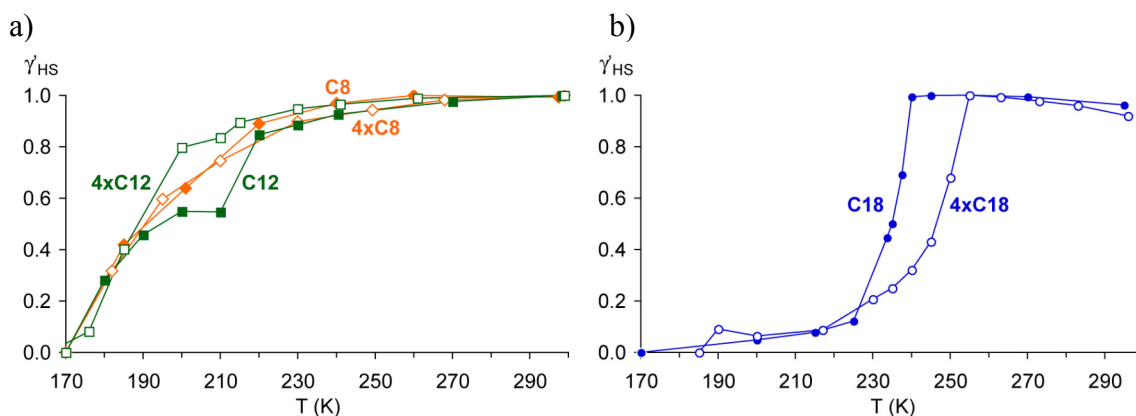


**Figure S6.** Fraction of HS complex  $\gamma_{HS}(T)$  for complexes with two and four alkyl chains, revealing no marked effect for short chains (Figure S5a: **1c**  $\blacklozenge$ , **2c**  $\blacklozenge$ , **1d**  $\blacksquare$ , **2d**  $\square$ ), yet a substantial influence when C<sub>18</sub>H<sub>37</sub> chains are introduced (Figure S4b: **1e**  $\bullet$ , **2e**  $\circ$ ); all 0.2 mM CH<sub>2</sub>Cl<sub>2</sub> solutions.

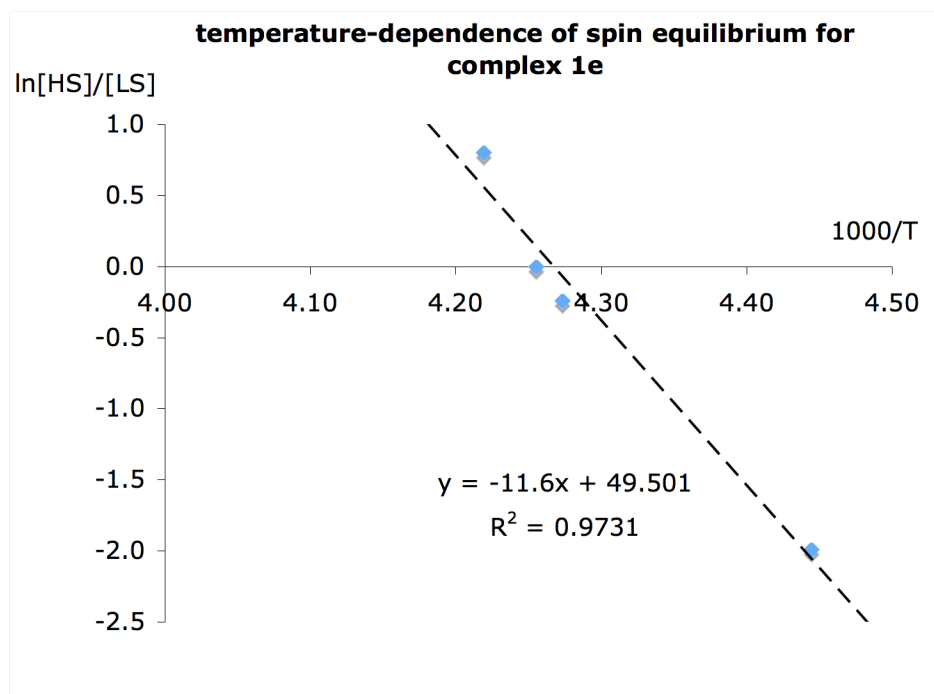


**Figure S7.** Van't Hoff plot of the logarithm of the spin equilibrium vs. the reciprocal temperature ( $\blacklozenge$ ), revealing a linear relationship. The ground state  $\Delta H^\circ$  and  $\Delta S^\circ$  values were extracted by least-square linear regression (dashed line).